Journal of Minerals and Materials Characterization and Engineering, 2020, 8, 84-96
https://www.scirp.org/journal/jmmce
ISSN Online: 2327-4085
ISSN Print: 2327-4077

The Potentials of Kyanite Particles and Coconut Shell Ash as Strengthener in Aluminum Alloy Composite for Automobile Brake Disc

Simon Godenaan Datau[1], Mohammed Ahmed Bawa[2], Jacob Shekwonudu Jatau[2], Muhammad Hamisu Muhammad[2], Adekunle Sefiu Bello[3]

[1]Department of Mechanical Engineering, University of Jos, Jos, Nigeria
[2]Department of Mechanical/Production Engineering, Abubakar Tafawa Balewa University, Bauchi, Nigeria
[3]Department of Materials Science and Engineering, Kwara State University, Malete, Nigeria
Email: simon.datau@yahoo.co.uk

How to cite this paper: Datau, S.G., Bawa, M.A., Jatau, J.S., Muhammad, M.H. and Bello, A.S. (2020) The Potentials of Kyanite Particles and Coconut Shell Ash as Strengthener in Aluminum Alloy Composite for Automobile Brake Disc. *Journal of Minerals and Materials Characterization and Engineering*, **8**, 84-96.
https://doi.org/10.4236/jmmce.2020.83006

Received: March 11, 2020
Accepted: April 13, 2020
Published: April 16, 2020

Abstract

The use of waste materials to produce engineering components is currently attracting so much interest due to their low cost, availability and environmental impact. In this study, coconut shell ash (CSA) and kyanite particles (KP) produced from coconut shells and kyanite mineral respectively were characterized. X-ray Florence (XRF), X-ray diffractometer (XRD) and scanning electron microscope (SEM) were used to analyze the oxide compositions, crystalline phases and microstructures of CSA and KP. The XRF analysis revealed major oxides in CSA and KP as SiO_2 and Fe_2O_3; and Al_2O_3 and SiO_2 respectively. The XRD analysis revealed the presence of Quartz, Hematite, Andradite and Gaultite phases at major peaks in diffractogram of CSA; and Quartz and Beryl phases at major peaks in the diffractogram of KP. The crystallite sizes of the quartz phases in CSA and KP at diffraction angle of 26.72˚C and 20.91˚C were determined as 638.28 Å and 789.38 Å respectively. From the SEM image of CSA, it was observed that particles of different sizes are present in the microstructure of CSA. The average size of the particles in the microstructure of CSA is 26.24 μm. A similar result was observed in the SEM image of KP and average size of the particles is 3.074 μm. Also, the energy dispersive X-ray (EDX) spectrums of CSA and KP revealed the presence of many elements with calcium as the major element in CSA and Aluminium as major element in KP. The presence of the crystalline phases in CSA (SiO_2, Al_2O_3, andradite, gaultite and hematite) and KP (SiO_2 and Al_2O_3) will make them good strengthening materials for the production of Aluminium based composites that can be used in applications where a good combination of strength and wear characteristics is a basic requirement like brake disc.

Keywords

Kyanite Particles, Coconut Shell Ash, Oxide Compounds, Crystalline Phases, Density and Strengtheners

1. Introduction

Waste materials (metal scraps, plastic and crop) are materials that are discarded as refuse. They are mostly generated from food and crop processing either as solid or liquid waste [1] [2] [3]. In developing countries, proper management of wastes remains a big challenge. Wastes are burned in the open with resultant environmental pollution due to emission of gases [4] [5] [6] [7].

In Nigeria, wastes are generated daily in the cities due to diverse human activities, yet only few states provide dumpsites. These wastes include: cartons, papers, animals bones, plastics, aluminium plates, nylon bags, ceramics, vegetable stems, electronics, computers, photocopiers, aluminium cans, etc. Nigeria is the biggest contributors to solid waste in Africa with an estimated 32 million tons per year [8] [9] [10] [11] [12].

Coconut shell wastes are produced in large quantity in most tropical countries worldwide as Coconut forms a regular part of the human diets and other uses: food, drinks, oil, decorations, charcoal, cosmetics, etc. In Kumasi, Ghana, 91% of the 4.5 tonnes of coconut wastes produced monthly are abandoned as refuse [13] [14] [15]. In Nigeria, coconut is produced in a large quantity; and in 2017, Nigeria was ranked 18th in the world with a production capacity of 288,615 tonnes behind Ghana that produced 366,183 tonnes [16].

Some studies recommended the use of coconut shell ash (CSA) as reinforcing material in place of silicon carbide (SiC) and aluminium oxide (Al_2O_3) because it is cheap, light, and contains oxides such as silicon oxide (SiO_2), Al_2O_3, magnesium oxide (MgO), iron oxide (FeO), etc. that have been used to strengthen metal matrix composites [13] [14]. Also, studies on the physical and chemical characteristics of the rice husk, palm kernel shell, coconut shell, wood sawdust, palm oil fibre, fly ash, and groundnut shell showed similar oxide compositions. The apparent density, total ash content, moisture content, particle size distribution and average particle size distribution were found to fall within the range recommended by ASTM [17] [18] [19].

Coconut shell ash was reported to be good filler in concrete mix as it contained carbon, silicon dioxide, potassium oxide, etc. [18] [19]. The apparent densities and particle sizes of carbonized and uncarbonized coconut shell were found to decrease with increase in milling time. The average particle sizes were reported as 50.01 nm (uncarbonized) and 14.29 nm (carbonized) for the milling time of 70 hours. Reduction in the volatiles content of the shell enhanced hardness [20] [21] [22].

Kyanite, on the other hand, is a mineral resource that exists in commercial

quantity in Niger and Kaduna [23]. It is mostly found in aluminium-rich metamorphic pegmatites and has a chemical formula $Al_2O_3 \cdot SiO_2$. It is used to produce heat resistant ceramics, abrasives, plumbing fixtures and high-temperature furnaces because of its high, hardness and decomposition temperature of 4 - 7 HV and 1380˚C [24] [25] [26] [27] [28].

A study on the Geochemistry and Mineralogy of Kyanite revealed that Al_2O_3 and SiO_2 constitute 92%. This confirms the suitability of Kyanite for use as reinforcing material [29].

The purpose of this study is to explore the potentials of kyanite particles and coconut shell ash as strengtheners in AMC as alternatives to Al_2O_3 and SiC in view of the fact that they contained SiO_2, Al_2O_3, MgO, FeO, etc.

2. Experimental Methodology

2.1. Production of the Coconut Shell Ash

The coconut shells were sourced, cleaned and dried for 2 days, and crushed into smaller particles using a crusher. The crushed particles (**Figure 1(a)**) was sieved to fine powder using a 300 mesh screen of size 53 μm. 10 g of the shell powder was weighed and placed in a small graphite crucible. The crucible was placed in an electric resistance furnace and fired at 1200˚C for 6 hours to form CSA. The ash, shown in **Figure 1(b)**, was again sieved to size 53 μm using a 300 mesh screen.

2.2. Production of Kyanite Particles

The Kyanite mineral (**Figure 2(a)**) was sourced and pulverized to form kyanite particles (KP) in the Material Processing Laboratory. The KP was sieved by passing it through a 300 mesh screen of size 53 μm and is as shown in **Figure 2(b)**.

2.3. Characterization of CSA and KP

2.3.1. Density

First, the Pycnometer bottle (**Figure 3**) was washed using distilled water and allowed to dry. Then the following weights: dry empty bottle (W_1); bottle with

(a) (b)

Figure 1. (a) Crushed coconut shell powder and (b) Coconut shell ash.

(a) (b)

Figure 2. (a) Kyanite material; (b) Kyanite particles.

Figure 3. Pycnometer bottle for density test.

CSA (W_2); bottle with CSA and water (W_3); and bottle with water (W_4) were determined. This procedure was repeated for KP.

Then Equation (1) was used to evaluate the density of CSA and KP [30]:

$$\rho = \frac{W_2 - W_1}{\{(W_4 - W_1) - (W_3 - W_2)\}} \times \text{density of water} \tag{1}$$

$$\rho_{\text{CSA}} = \frac{51.316 - 37.648}{(87.135 - 37.648) - (95.862 - 51.316)} \times 1.0 = 2.7662\,\text{g/cm}^3$$

$$\rho_{\text{KP}} = \frac{45.342 - 37.604}{(87.137 - 37.604) - (92.499 - 45.342)} \times 1.0 = 3.2567\,\text{g/cm}^3$$

2.3.2. Thermal Conductivity

10 g each of CSA was ground to very fine powder and liquid binder were added; then homogenized gently using a small mortar and pestle until the CSA turned to powder form. The prepared CSA was compacted to cylindrical specimens using a hydraulic press and specimen (**Figure 4**) was placed in Searle's apparatus to measure the thermal conductivity. This procedure was repeated for the KP.

Equation (2) was used to evaluate the thermal conductivity of CSA and KP.

$$K = \frac{QL}{A(T_2 - T_1)} \tag{2}$$

where: Q = heat (w); L = length or thickness of the specimen (m); A = cross-sectional area of the specimen; $T_2 - T_1$ = temperature gradient (K).

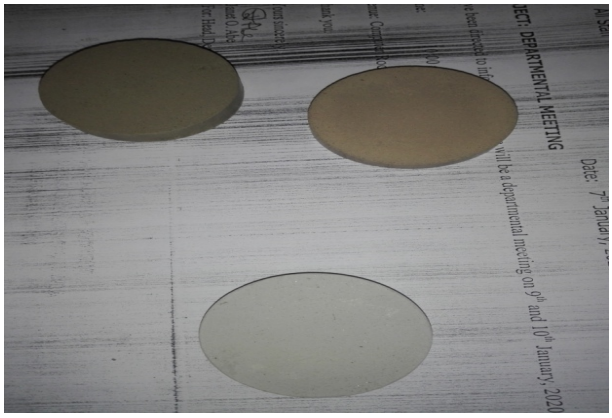

Figure 4. CSA and KP specimens.

2.3.3. Oxide Compounds

The XRF was used to determine the Oxide compounds present in the CSA and KP. 10 g of CSA was placed in agate mortar and 1 g of stearic acid (binder) was added and the mixture thoroughly homogenized. The homogenized CSA was placed in a hardened steel disc and pressed into a pellet using hydraulic pressure press. Minipal 4 EDXRF at National Geoscience Research Laboratory was used to analyze the pellets. This procedure was repeated for the prepared specimen of KP.

2.3.4. Crystallaline Phases

Empyrean XRD Spectrometer was used to determine the crystalline phases present in CSA and KP. 10 g of CSA was placed in a specimen holder and pressed. The specimen was placed in the spectrometer and the test parameters (diffraction angles) inputted through a computer system connected to the spectrometer. The measurement conditions were copper target operated at 40 keV and 30 mA, with a continuous scan mode in the range of 2˚ to 80˚ and drive axis of Theta-2-Theta. This procedure was repeated for 10 g of KP. The results are presented in **Figure 5** and **Figure 6** respectively.

The size of crystallite at the major peaks in the XRD profiles of CSA and KP was determined using Scherrer's equation shown below:

$$D = \frac{0.9\lambda}{\beta \cos\theta} \tag{3}$$

where D = particle size; λ = wavelength of CuKa1 radiation = 1.54060 Å; d = full width at half maximum intensity of the peak (in radians); θ = half diffraction angle; β = constant = 0.9

The size of the crystallite particle at 2θ of 21.7194˚C for CSA was determined as thus:

$$D = \frac{0.9 \times 1.5406}{2.233 \times 10^{-3} \cos 13.3597} = 638.28 \text{ Å}$$

2.3.5. Crystal Structure Analysis

5 g of CSA was used for the analysis. A double sided adhesive pad was attached

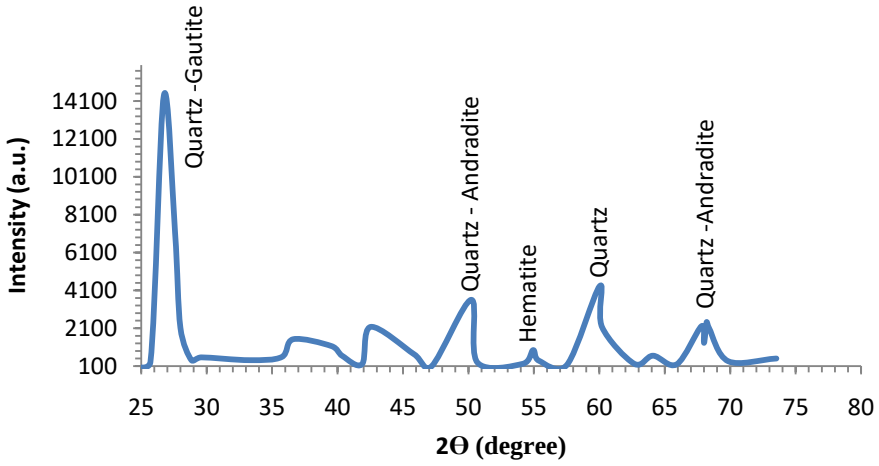

Figure 5. XRD profile of CSA.

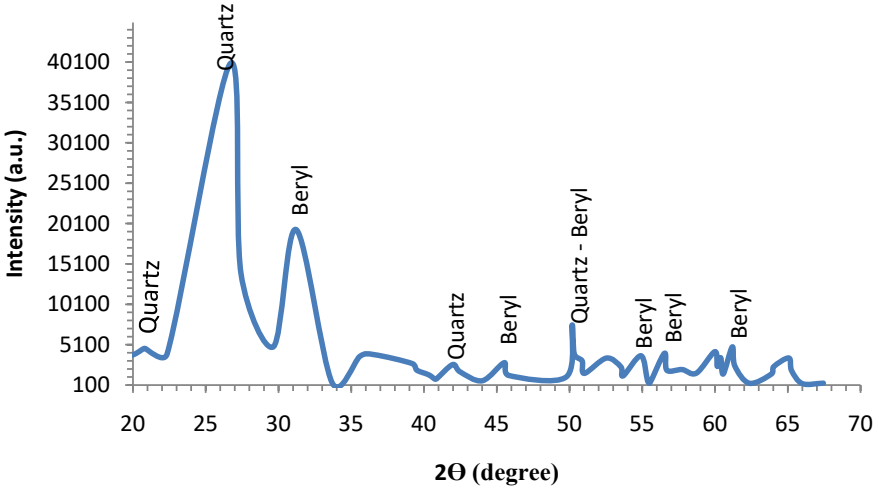

Figure 6. XRD profile for KP.

to a bare specimen stub. Then the specimen was collected on the tip of a toothpick and the coated tip brushed against the expose adhesive of the specimen stub. The particles were pressed firmly against the adhesive pad. The stub containing the specimen was griped in place using a tweezer and then taped forcibly on the side of a table or bench to remove loose particles from the specimen stub. The specimen was placed in the Phenom SEM, and the specimen was transferred automatically to the optical imaging position. The optical camera was activated and the image was displayed in the main viewing window of the image screen. The brightness and magnification of the optical image were adjusted. The SEM image of CSA is shown in Figure 5. The procedure was repeated using 10 g of KP and SEM image is presented in Figure 6.

3. Results and Discussion

3.1. Density of CSA (ρ_{CSA}) and KP (ρ_{KP})

The densities of CSA and KP are presented in Table 1.

Table 1. Density of CSA and KP.

ρ_{CSA} (g·cm^{-3})	ρ_{KP} (g·cm^{-3})
2.77	3.26

The results showed that CSA and KP are light materials. The density of the kyanite particle is higher than that of coconut shell ash. This perhaps is due to the high concentrations of Al_2O_3 and SiO_2 in kyanite particles compare to that in coconut shell ash. These densities fall within the range of densities of some ashes (fly ash, rice husk ash, groundnut shell ash, silica, etc.): 1.8 to 3.5 g·cm^{-3}.

3.2. Thermal Conductivity of CSA and KP

Thermal conductivity (TC_{CSA}) of CSA and KP (TC_{KP}) are shown in **Table 2**.

The thermal conductivity of KP is higher than that coconut shell ash. This is attributed to the high concentration of aluminium in KP. This is in agreement with thermal conductivities of the ashes of most crop wastes which are generally low [18] [19].

3.3. Oxide Compounds Present in CSA and KP

The oxide compounds present in CSA and KP were obtained through XRF analysis and the results are presented in **Table 3**.

From **Table 3**, the major oxides present in CSA and KP are SiO_2, Al_2O_3, Fe_2O_3 and CaO. SiO_2 is major in CSA while Al_2O_3 is major oxide in KP. The higher concentrations of Al_2O_3 and SiO_2 particles in kyanite particles confirm the fact that is a compound of aluminium silicate [24] [25] [26] [27]. The oxides of CSA are similar to that presented by [17].

3.4. Crystalline Phases Present in CSA and KP

The different crystal phases present in CSA and KP are shown in **Figure 5** and **Figure 6**.

Figure 5 showed the intensity of the different crystalline phases present in CSA. The crystalline phases are Quartz-Gaulite, Quartz-Andradite, Hematite, Quartz, and Quartz-Andradite at respective diffraction angles (2θ) of 26.62˚, 49.20˚, 55.0˚, 59.06˚ and 69.01˚. The respective inter-planar spacing is 3.34, 2.69, 3.01 and 6.38 Å. The standard reference codes that matched the phases in the CSA are presented in **Table 4**. The amounts (in percent) of Quartz, Hematite, Andradite and Gautiteare61.6%, 1%, 18.2% and 19.2% respectively; revealed quartz to be the major Phase.

Figure 6 presents the intensity of the different crystalline phases in KP. The peaks indicated quartz and beryl when matched with standard codes. At diffraction angles (2θ) of 26.62˚ and 31.03˚, the peaks are Quartz and Beryl at respective inter-planar spacing is 3.34 and 7.98 Å. The amount of quartz and beryl in KP are 64% and 36% respectively. The standard reference codes that matched the crystalline phases in KP are as shown in **Table 5**.

Table 2. Thermal conductivity of CSA and KP.

TC_{CSA} ($Wm^{-1}\cdot k^{-1}$)	TC_{KP} ($Wm^{-1}\cdot k^{-1}$)
0.891	1.111

Table 3. Oxide compounds of CSA and KP (%).

Compound	CSA (%)	KP (%)
SiO_2	25.14	47.10
TiO_2	2.38	01.15
Al_2O_3	10.23	48.60
Fe_2O_3	23.17	0.496
SO_3	5.90	-
CaO	18.20	0.14
MgO	2.80	0.013
Na_2O	5.69	0.105
K_2O	3.10	0.13
Cl	1.20	-
MnO	0.20	0.02
V_2O_5	0.048	0.028
Cr_2O_3	0.068	<0.001
CuO	0.476	0.03
ZnO	0.476	0.006
SrO	0.28	0.04
BaO	0.65	-
L.O.I	-	2.14

Table 4. Reference codes of standards that matched the crystal phases in CSA.

Ref. Code	Score	Compound name	Chem. Formula
96-901-0146	72	Quartz	Si_6O_6
96-900-9783	42	Hematite	$Fe_{12}\ O_{18}$
96-900-1254	29	Andradite	$Ca_{12}\ Fe_{7.54}Si_{12}O_{48}$
96-900-4338	18	Gaultite	$Zn_{16}Si_{56}\ Na_{32}O_{192}H_{64}$

Table 5. Standard reference codes that matched the phases in KP.

Ref. Code	Score	Compound name	Chem. Formula
96-900-9667	65	Quartz	Si_3O_6
96-900-1555	72	Beryl	$Si_{12}Be_6Al_{3.94}Fe_{0.06}O_{36.48}Na_{0.03}H_{0.52}$

The presence of Quartz and Beryl will make KP suitable for use as a strengthening material for the production of metal composites.

The sizes of crystallites at the major peaks of the XRD profile of CSA and KP were determined using Scherrer's equation shown below:

$$D = \frac{0.9\lambda}{\beta \cos\theta} \tag{4}$$

where D = particle size; λ = wavelength of CuKa1 radiation = 1.54060 Å; β = full width at half maximum intensity of the peak (in radians); θ = half diffraction angle.

The size of the crystallite at 2θ of 20.9134˚and β = 0.1023˚ was determined as follows:

$$D = \frac{0.9 \times 1.5406}{1.7862 \times 10^{-3} \cos 10.4567} = 789.377 \text{ Å}$$

3.5. Microstructures of CSA and KP

The microstructures and energy dispersive spectrographs of the CSA and KP determined through SEM and Energy dispersive X-ray analysis respectively are presented in Figure 7 and Figure 8.

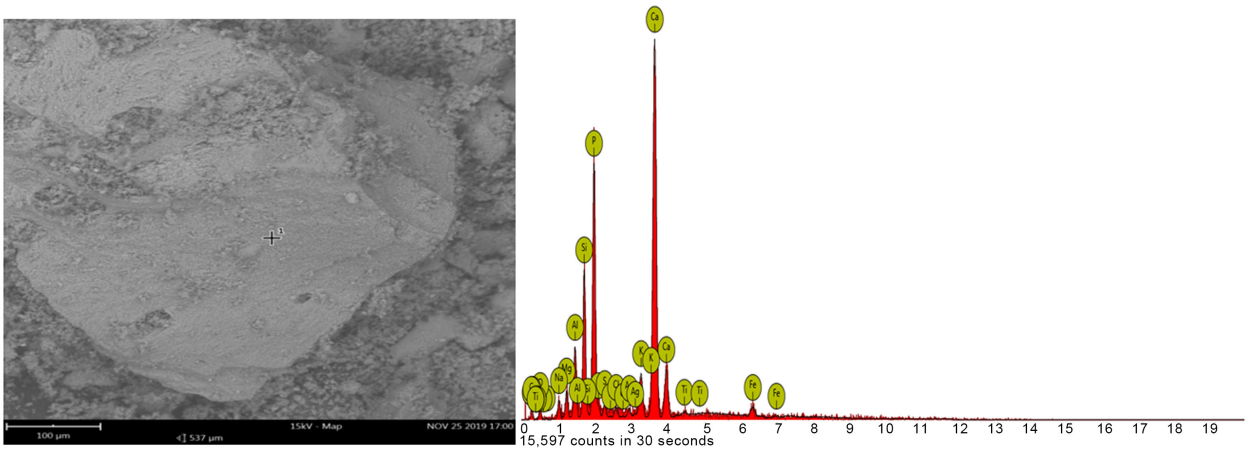

Figure 7. SEM image and EDX spectrograph of CSA.

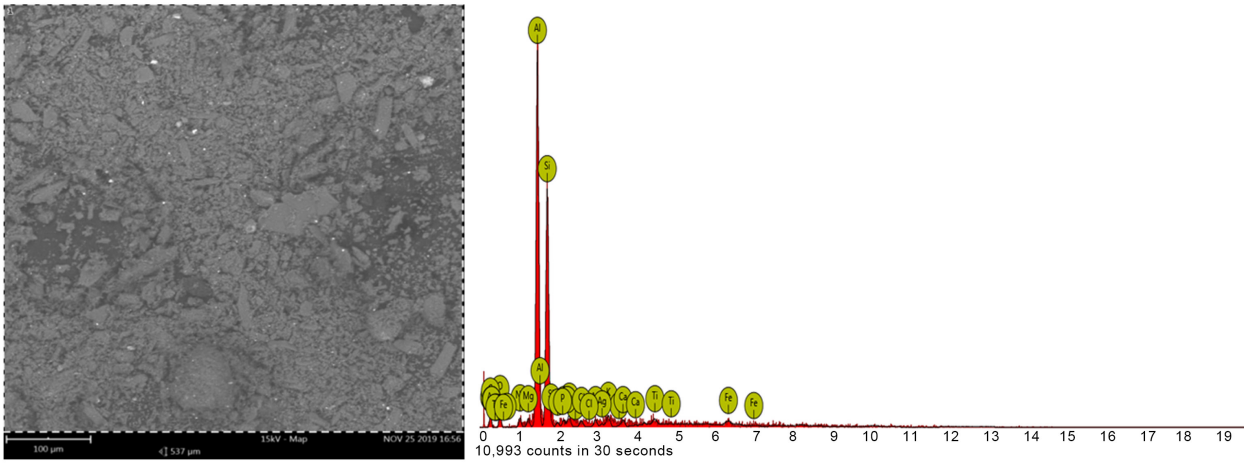

Figure 8. SEM/EDS of kyanite particles.

The SEM image of CSA presented in Figure 7 above revealed the presence of particles of different sizes. The microstructure of the produced CSA is not uniform. This perhaps is due to the presence of the crystalline phases (quartz, andratite, gaultite and hematite) in the ash. Also, the EDX spectrograph of the CSA revealed the presence of the following elements: calcium (Ca), phosphorus (P), silicon (Si), carbon (C), oxygen (O), iron (Fe), potassium (K), aluminum (Al), magnesium (Mg), silver (Ag), sodium (Na), sulphur (S), chlorine (Cl) and titanium (Ti); with Ca having the highest intensity. The presence of these elements showed that CSA has no radioactive and as such it is not toxic.

Like the SEM image of CSA, the SEM image of KP presented in Figure 8 above showed non-uniform microstructure. Particles of different sizes are observed to be present in the microstructure of KP. Perhaps, this is due to the presence of the crystalline particles (quartz and beryl) in KP. Also, the EDX spectrograph revealed the presence of the following elements: Al, Si, C, O, Mg, Ag, Nb, K, Ti, Ca, Cl, S, Na, P and Fe; with Al having the highest intensity.

3.6. Particle Sizes of CSA and KP

Imaging particle sizes of CSA and KP obtained from SEM images of CSA and KP (Figure 7 and Figure 8) are presented in Figure 9 and Figure 10. Tomography

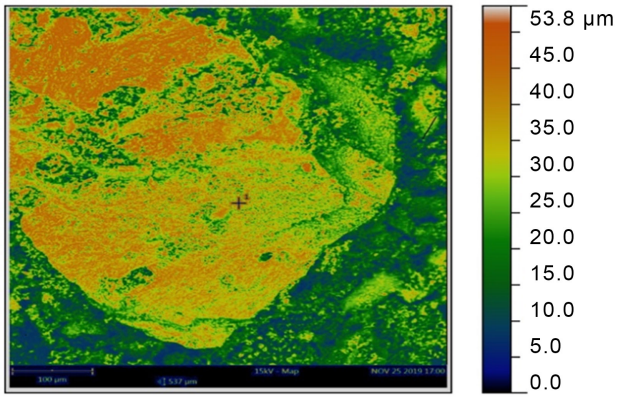

Figure 9. Particle size of CSA.

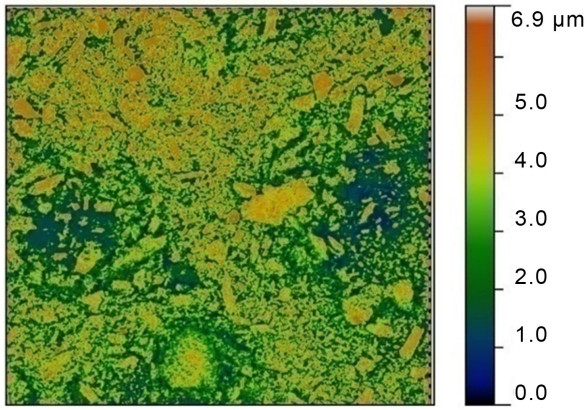

Figure 10. Particle size of KP.

in Figure 9 and Figure 10 showed that the average particles sizes of CSA and KP are 26.42 μm and 3.074 μm respectively.

4. Conclusions

The following conclusions were made based on the production and characterization of coconut shell ash and kyanite particles.

1) The densities of CSA and KP showed CSA and KP are light materials.

2) The XRF analysis revealed SiO_2, Al_2O_3 and Fe_2O_3 as major oxides in CSA while SiO_2 and Al_2O_3 as major oxides in kyanite particles. The presence of these hard particles will make CSA and KP suitable for use as reinforcements for the production of Al composites.

3) The XRD analysis revealed Quartz, Hematite, Andradite and Gaultite as crystalline phases in CSA; and Quartz and Beryl as crystalline phases in KP. The quantity of the phases in CSA are Quartz (61.6%), Andradite (18.2%), Gaultite (19.2%) and Hematite (1%) while in KP Quartz and Beryl are 64% and 36% respectively.

4) The crystallite size quartz at 2θ of 26.7194˚C in XRD profile of CSA is 638.28 Å; while that quartz at 2θ of 20.9134˚C in the XRD profile of KP is 789.38 Å

5) The average particle sizes in the microstructures of CSA and KP are 26.42 μm and 3.074 μm. These will enhance strengthening when used as reinforcing material. No radioactive element was revealed by the EDX of CSA and KP.

Conflicts of Interest

The authors declare no conflicts of interest regarding the publication of this paper.

References

[1] Anyanwu, C.N., Ibeto, C.N., Eze, I.S. and Ezeoha, S.L. (2013) Present and Prospective Energy Use Potentials of Selected Agricultural Wastes in Nigeria. *Journal of Renewable and Sustainable Energy*, **5**, Article ID: 032703. https://doi.org/10.1063/1.4808046

[2] Rosenkranz, A., Pichelin, F., Lehman, M., Job, C., Kimeng, H.T., Mustapha, S., *et al.* (2011) Nigerian Agricultural Waste Products for the Production of Particleboard. *Conference Paper on Science & Technology of Biomass*: *Advances and Challenges*, 5-8.

[3] Oladepo, O.W., Ilori, M.O. and Taiwo, K.A. (2015) Assessment of the Waste Generation and Management Practices in Nigerian Food Industry: Towards a Policy for Sustainable Approaches. *American Journal of Scientific and Industrial Research*, **6**, 12-22.

[4] Andreas, B. (2014) Moving from Recycling to Waste Prevention: A Review of Barriers and Enables. *Waste Management & Research*, **32**, 3-18. https://doi.org/10.1177/0734242X14541986

[5] Davies, B.O. (2015) Conversion of Agricultural Wastes into Poultry Feed for Sustainable Environment. Master's Thesis, Federal University of Technology, Owerri.

[6] Adeyi, O. (2010) Proximate Composition of Some Agricultural Wastes in Nigeria and Their Potential Use in Activated Carbon Production. *Journal of Applied Science and Environmental Management*, **14**, 55-58. https://doi.org/10.4314/jasem.v14i1.56490

[7] Iorhemen, O.T., Meshach, I.A. and Onoja, S.B. (2016) The Review of Municipal Solid Waste Management in Nigeria: The Current Trends. *Advances in Environmental Research*, **5**, 237-249. https://doi.org/10.12989/aer.2016.5.4.237

[8] Obi, F.O., Ugwuishiwu, B.O. and Nwakaire, J.N. (2016) Agricultural Waste Concept, Generation, Utilization and Management. *Nigerian Journal of Technology*, **35**, 957-964. https://doi.org/10.4314/njt.v35i4.34

[9] Akindayo, A.S. (2019) Municipal Solid Waste Management and the Inland Water Bodies: Nigerian Perspectives.

[10] Babayemi, J.O. and Dauda, K.T. (2009) Evaluation of Solid Waste Generation, Categories and Disposal Options in Developing Countries: A Case Study of Nigeria. *Journal of Applied Science and Environmental Management*, **13**, 83-88. https://doi.org/10.4314/jasem.v13i3.55370

[11] Konya, R.S., Zitte, L.F. and Ugwulor, Q.N. (2013) Characterization of Wastes and Their Recycling Potentials; A Case Study of East-West Road, Port Harcourt. *Journal of Applied Science and Environmental Management*, **17**, 233-238. https://doi.org/10.4314/jasem.v17i2.7

[12] Salami, H.A., Adegite, J.O., Bademosi, T.T., Lawal, S.O., Olutayo, O.O. and Olowosokedile, O. (2018) A Review on the Current Status of Municipal Solid Waste Management in Nigeria: Problems and Solutions. *Journal of Engineering Research and Reports*, **3**, 1-16. https://doi.org/10.9734/jerr/2018/v3i416884

[13] Ofori-Agyeman, C. (2016) Assessment of Quantity of Coconut Waste Generated and Management in the Kumasi Metropolis, Ghana. Kwame Nkrumah University of Science and Technology College of Engineering, Ghana.

[14] Ibrahim, Y. and Mohammed, Z.G. (2018) The Potential of Coconut Shell as Biofuel. *The Journal of Middle East and North Africa Sciences*, **4**.

[15] Romulo, N.A. (2013) Market and Trade of Coconut Products. Asian and Pacific Coconut Community, Thailand, 1-122.

[16] The Food and Agriculture Organization Corporate Statistical Database, FAOSTAT (2017) Coconut Production in Nigeria from 1961-2017.

[17] Madakson, P.B., Yawas, D.S. and Apasi, A. (2012) Characterization of Coconut Shell Ash for Potential Utilization in Metal Matrix Composites for Automotive Applications. *International Journal of Engineering Science and Technology*, **4**, 1190.

[18] Lancaster, L., Lung, M.H. and Sujan, D. (2013) Utilization of Agro-Industrial Waste in Metal Matrix Composites: Towards Sustainability. *International Journal of Environmental, Chemical, Ecological, Geological and Geophysical Engineering*, **7**, 25-33.

[19] Wan, W.A., Ghani, A.K., Abdullah, M.S.F., Matori, K.A., Alias, A.B. and Silva, G.D. (2010) Physical and Thermo-Chemical Characterisation of Malaysian Biomass Ashes. *Journal of the Institution of Engineers*, **71**, 9-18.

[20] Tay, L.T., Ramadhansyah, P.J., Norhidayah, A.H., Haryati, Y., Dewi, S.J. and Mohd, A.M.A. (2016) A Review of Chemical and Physical Properties of Coconut Shell in Asphalt Mixture. *Jurnal Teknologi* (*Sciences & Engineering*) **78**, 85-89. https://doi.org/10.11113/jt.v78.8002

[21] Olowoyo, D.N. and Orere, E.E. (2012) Preparation and Characterization of Activated Carbon Made from Palm-Kernel Shell, Coconut Shell, Groundnut Shell and

Obeche Wood (Investigation of Apparent Density, Total Ash Content, Moisture Content, Particle Size Distribution Parameters). *International Journal of Research in Chemistry and Environment*, **2**, 32-35.

[22] Lalit, K., Kamal, K.P. and Sabir, K. (2017) Use of Coconut Shell Ash as Aggregates. *International Journal of Research in Engineering and Social Sciences*, **7**, 15-19.

[23] Nigeria Investment Promotion Commission (2019) Solid Mineral in Nigeria.

[24] Alif, S.L., Shahiron, S., Mohamad, S.S. and Nuru, I.R.R.H. (2016) A Preliminary Study on Chemical and Physical Properties of Coconut Shell Powder as a Filler in Concrete. *IOP Conference Series*: *Materials Science and Engineering*, **640**, Article ID: 012059. https://doi.org/10.1088/1757-899X/160/1/012059

[25] Bello, S.A., Agunsoye, J.O., Adebisi, J.A., Kolawole, F.O. and Hassan, S.B. (2016) Physical Properties of Coconut Shell Nanoparticles. *Kathmandu University Journal of Science*, *Engineering & Technology*, **12**, 63-79. https://doi.org/10.3126/kuset.v12i1.21566

[26] Apasi, A., Yawas, D.S., Abdulkareem, S. and Kolawole, M.Y. (2016) Improving Mechanical Properties of Aluminium Alloy through Addition of Coconut Shell Ash. *Journal of Science and Technology*, **36**, 34-43.

[27] Li, W. (2008) Effects of Carbonization Temperatures on Characteristics of Porosity in Coconut Shell Chars and Activated Carbons Derived from Carbonized Coconut Shell Chars. *Industrial Crops and Products*, **28**, 190-198. https://doi.org/10.1016/j.indcrop.2008.02.012

[28] Olade, M.A. (2019) Solid Mineral Deposits and Mining in Nigeria: A Sector in Transitional Change. *Achievers Journal of Scientific Research*, **2**, 1-16.

[29] Omang, B.O. and Alabi, A.A. (2011) Geochemistry and Mineralogical Evaluation of Quartzite Bearing Kyanite in Kuta, North-Western Nigeria. *Ethiopian Journal of Environmental studies and Management*, **4**, 79-83. https://doi.org/10.4314/ejesm.v4i3.11

[30] Sayatu, M., Sulaiman, S., Vijayaram, T.R., Baharudin, B.T.H.T. and Arifin, M.K.A. (2012) Manufacturing and Properties of Quartz (SiO_2) Particulate Reinforced-Al-11.8%Si Matrix Composites.